PFC/JA-96-47

High Power Operation of a 170 GHz Gyrotron for ITER

K.E. Kreischer, T. Kimura, B.G. Danly*, and R.J. Temkin

November, 1996

Plasma Fusion Center
Massachusetts Institute of Technology
Cambridge, MA 02139

*Present Address: Naval Research Laboratory, Code 6843, Washington D.C., 20375

This work was supported by the U.S. Department of Energy, Grant No. DE-FC02-93ER54186. Reproduction, translation, publication, use and disposal, in whole or in part, by or for the United States government is permitted.

Submitted for publication in : Physics of Plasmas.

High Power Operation of a 170 GHz Gyrotron for ITER

K.E. Kreischer. T. Kimura, B.G. Danly*, and R.J. Temkin

Plasma Fusion Center, Massachusetts Institute of Technology, Cambridge, MA 02139

ABSTRACT

Recent megawatt gyrotron experiments at MIT have achieved record powers at 170 GHz. Single mode emission with a peak output power of 1.5 MW and an efficiency of 35% has been measured. The experiment is based on a resonant $TE_{28,8,1}$ cylindrical cavity situated in a 6.7 T magnetic field. Microwaves are generated in the cavity by an 83 kV annular electron beam produced by a triode-type magnetron injection gun that is capable of currents up to 50 A. Megawatt power levels with efficiencies between 30-36% have been measured over a wide range of operating parameters for the $TE_{28,8,1}$ mode. Similar results were also achieved in the neighboring $TE_{27,8,1}$ mode at 166.6 GHz, and the $TE_{29,8,1}$ mode at 173.5 GHz. The high output power is the result of a carefully designed electron gun with low perpendicular velocity spread (6-10%) and a novel cavity with an output iris that is less prone to mode competition. These results are in good agreement with nonlinear multimode simulations.

PACS: 84.40.I, 52.50.G, 07.57.H, 84.40.F

*Present Address: Naval Research Laboratory, Code 6843, Washington D.C., 20375

I. INTRODUCTION

The gyrotron[1] was first proposed as a high frequency device in the 1950's, and has since developed into a powerful source of microwaves. The high average power capability of gyrotrons is particularly evident in the millimeter and submillimeter wave region when compared to conventional tubes such as klystrons and traveling wave tubes (TWT's). A large variety of experiments over the past ten years have demonstrated that gyrotrons are capable of megawatt power levels at frequencies of 100 GHz and above. In the U.S., researchers at C.P.I.[2] working at 110 GHz with a $TE_{22,6,1}$ mode cavity have achieved output powers of 680, 530, and 350 kW for pulse durations of 0.5, 2.0, and 10.0 s respectively. There is also a significant international gyrotron research effort, primarily motivated by the need for long pulse oscillators for fusion plasma heating. Notable oscillator experiments include efforts at 84[3], 110[4], 118[5], and 140[6] GHz that have produced powers between 0.5-1.0 MW for pulse lengths of 0.2-5.0 s.

The gyrotron is a fast wave device that relies on a cyclotron resonance interaction between an electron beam and rf fields in a TE-mode cavity to generate microwaves. This synchronism is maintained by an axial magnetic field, and as a result a simple, cylindrical resonator capable of high power can be used. This is in contrast to conventional slow-wave devices, such as the TWT, that are prone to overheating or breakdown at high frequencies because of the small coupling structures that are required. The gyrotron operates with the cavity near cutoff, and as a result its interaction efficiency is less sensitive to beam velocity spread than other fast wave devices such as the free electron laser (FEL). However, because the gyrotron operates near cutoff, the rf fields in the cavity are very intense, and thermal heating of the cavity walls becomes a limiting factor when high powers are generated.

A variety of potential applications have motivated the development of gyrotron oscillators and amplifiers, including high resolution radar, particle acceleration, material processing, and plasma diagnostics. Certainly one of the strongest motivations has been the need for powerful millimeter wave sources for electron cyclotron resonance heating (ECRH) of fusion plasmas. Recent experiments on both tokamaks and stellarators[7] have demonstrated that efficient heating with local deposition of the power is possible with ECRH. Plasma heating requires efficient gyrotron oscillators capable of producing high average power in a single, high frequency mode.

The next major fusion experiment now being planned is the collaboration known as the International Thermonuclear Experimental Reactor (ITER). This device will produce over 1000 MW of fusion power, and auxiliary heating will be essential for accessing the H-mode and reaching ignition. ECRH utilizing gyrotrons is a strong contender for this role[8], and is being considered for a variety of functions including plasma breakdown, bulk heating, and current drive. Frequencies between 140 and 200 GHz will be needed depending on the function. Because of the large size of the planned ECRH system (up to 100 MW), individual gyrotrons must produce at least 1 MW. System costs will be important, so each unit will need to achieve an interaction efficiency greater than 35%.

To circumvent the wall thermal problems associated with operating near cutoff, gyrotrons typically utilize highly overmoded cavities. To determine a suitable mode for a given power P and frequency ν, one must determine the energy balance within the cavity, and from this calculate the equilibrium rf fields. This leads to the following equation[9] for the mode index ν_{mp} of the TE_{mp} mode of a gyrotron cavity:

$$\left(\nu_{mp}^2 - m^2\right) = \frac{1.2\times10^{-3} LP(MW)\nu^{2.5}(GHz)}{\lambda(1-R_2)\rho_{ohm}(kW/cm^2)} \qquad (1)$$

In this equation L is the characteristic axial length of the rf field profile in the cavity, λ is the wavelength, R_2 is the reflection coefficient at the cavity output, and ρ_{ohm} is the peak ohmic heating density in the cavity walls. An electrical conductivity of 5.0×10^7 $(\Omega\text{–m})^{-1}$, corresponding to ideal conditions at room temperature, is assumed. In actual operation, the gyrotron cavity wall temperature can be as high as 250° C, and the resulting higher resistivity can increase the ohmic losses by about 50-70%. Equation (1) shows the tradeoff between power and frequency, and the strong dependence of the operating mode on frequency. This equation has been plotted in Figure 1 using L/λ of 6.5, which results in an efficient interaction between the beam and rf field, and a reflection coefficient R_2 of 0.5. It is clear from Fig. 1 that utilizing advanced cooling techniques that allow the highest values of ρ_{ohm} would be advantageous. However, tube reliability is also an issue, and excessive cavity wall temperatures can lead to problems such as cyclical fatigue. Past experience with long pulse gyrotrons have shown that peak ohmic losses of about 2 kW/cm^2 (ideal conditions) can be tolerated without degrading reliability. For 1 MW output powers at 170 GHz, Fig. 1 indicates that a mode with ν_{mp} greater than 50 is required.

At M.I.T. we are presently investigating gyrotron oscillators that will satisfy the needs of the ITER experiment. Our gyrotrons are typically operated for 3 μsec pulses at 2 Hz but are designed to model long pulse or cw operation. This allows us to study the physics of the interaction without the complications associated with high average power. We are particularly interested in characterizing operation in very high order TE modes, and determining if mode competition adversely affects the interaction efficiency as the gyrotron becomes more overmoded. Past experiments have suggested that the tapered cavity commonly used in gyrotrons becomes less effective when $\nu_{mp} \geq 40$, and that a more complicated structure with fewer modes would be needed. This has led to gyrotrons based on complex and coaxial cavities.

The first experiments at MIT[10,11] investigated the $TE_{0,3,1}$ and $TE_{15,2,1}$ modes at 140 GHz. Both gyrotrons were able to generate high powers, but initially had efficiencies below 30% at higher beam currents. Careful design of the cavities, and optimization of the operating parameters, eventually eliminated this problem in both cases. We later investigated very high order TE modes with ν_{mp} up to 75 in the 200-300 GHz range[12]. Efficiencies below 25% were measured at powers approaching 1 MW. We were unable to significantly improve this efficiency, and attributed our difficulties to poor beam quality and a tapered cavity with too many competing modes.

This paper describes the efforts at M.I.T. to demonstrate efficient gyrotron operation at 170 GHz with a tapered cavity. It is organized in the following manner. In Section II we will give an overview of the design of the experiment, focusing on our efforts to build an electron gun with very good beam quality. In Section III, we will present our measurements of the operation of the tube, including efficiency, observed modes, and startup characteristics. We will also compare these results with nonlinear theory. Conclusions and future plans will be discussed in Section IV.

II. DESIGN OF EXPERIMENT

This experiment was our first attempt to build a prototype of a 170 GHz megawatt gyrotron that would meet the needs of ITER. Therefore we decided to choose conservative design features that had been successfully demonstrated in past tests. The experiment was based on a cylindrical tapered cavity that has proven very successful in previous high power gyrotrons. Even though there was some concern about the cavity's effectiveness when operating in a very high order mode, we were able to mitigate this problem by keeping the interaction length short. A schematic of the 170 GHz gyrotron is shown in Figure 2. The experiment was operated with the tube in the horizontal position. A superconducting 7.5 T magnet built by Cryomagnetics, Inc., with a 20 cm warm bore provided the cavity magnetic field. The magnet consists of a pair of coils that allow tapering of the magnetic field in the cavity region. Such magnetic tapering has been used in the past to enhance the efficiency. However, the results presented in this paper were obtained with a flat field at the cavity. The large bore is needed to accommodate the mode converter and mirror transmission line inside the gyrotron. The magnet is fitted with a lambda plate, and can be operated up to 9 T by pumping on the liquid helium cryostat. This feature will allow us to investigate gyrotron operation above 200 GHz. A 0.3 T room-temperature gun coil attached to the magnet was used to adjust the electron beam radius and velocity ratio.

The overall design of the 170 GHz gyrotron is similar to that used in many previous experiments, including those at M.I.T. Parameters of this tube are given in Table I, and are based on peak cavity ohmic losses of 2.1 kW/cm^2 (ideal conditions, see Figure 1). The major differences of this experiment when compared to our previous research at 110 GHz[13] are the need to operate in a higher order mode, and the larger magnetic compression of the electron beam (36 versus 24). The annular beam is produced by a triode magnetron injection gun built by Communication and Power Industries (C.P.I., formerly Varian Associates). A beam with voltages up to 100 kV, and currents up to 50 A, can be produced. The drift region between the gun and cavity contains slotted structures to prevent spurious oscillations. In addition, there is a section 5 cm long just before the cavity consisting of alternating copper and Ceralloy rings that absorb any power leaking from the cavity that could reach the cathode region and disrupt gun operation. After magnetically compressing the beam in the drift region, its velocity ratio $\alpha=v_\perp/v_{||}$ ($v_\perp$ and $v_{||}$ are the beam's perpendicular and parallel velocity) at the cavity is 1.6. The beam radius R_e in the cavity was chosen so that the beam would couple to the inner radial maximum of the $TE_{28,8,1}$

mode. This corresponds to $k_{\perp}R_c$=29.45, where $k_{\perp}$ is the perpendicular wavenumber in the cavity. Positioning the beam on the inner radial maximum provides stronger coupling and less mode competition. The 0.86 cm separation between the beam and cavity wall is quite large, and results in a relatively high voltage depression of the beam (6 kV for a 35 A beam).

A major focus of this experiment was to design and construct a highly overmoded tapered cavity less affected by mode competition. In order to determine when competition would prevent operation at high efficiency, the cavity designs were simulated with a self-consistent, time-dependent multimode code developed at the University of Maryland[14]. We started with a simple profile consisting of a linear uptaper, straight section, and linear output taper. We lengthened the straight section in order to increase the diffractive Q to the desired value, but found that multimoding became a problem when L/λ exceeded 6.5. We therefore chose a relatively short straight section to ensure that L/λ did not exceed this value, but included an iris at the cavity output to raise the cavity diffractive Q to the desired value. The final design of the resonator consisted of the following dimensions: 3 degree linear input taper, 0.8 cm long straight section with a 5×10^{-3} cm iris step at the end, and a non-linear uptaper to 7% above the cutoff radius of the cavity. This cavity has a diffractive Q of 1300 based on cold cavity simulations, which is about 2.5 times larger than the minimum Q of $4\pi(L/\lambda)^2$. Operating well above the minimum Q is needed to achieve high efficiency, and helps to reduce the cavity's sensitivity to external reflections. The transition from the input taper to the straight section was rounded in order to minimize the mode conversion that could cause power leakage back into the gun region.. Mode conversion in the nonlinear uptaper was calculated to be less than 0.5%. Assuming a 10% perpendicular velocity spread and a beam velocity ratio of 1.6, an efficiency of 39% was predicted by multimode nonlinear theory for an 83 kV, 36 A beam, giving 1.2 MW of rf power generated in the cavity.

Taking into account ohmic and transmission losses inside the gyrotron and at the window reduces the power leaving the gyrotron to 1 MW, for an overall efficiency of 35%.

The high order TE modes generated by megawatt gyrotrons are difficult to transmit efficiently, and therefore an internal mode converter can typically be found in these devices. In our case the mode converter immediately follows the cavity, and is designed to transform the $TE_{28,8}$ mode into a Gaussian beam that can then be transported to the fusion plasma with corrugated waveguide. The converter[15] consists of a cylindrical launcher with small periodic wall perturbations and a four-mirror transmission line. The perturbations produce a mix of satellite modes that combine with the original mode to give a Gaussian-like beam. This beam is then launched through a slot in the launcher wall. Figure 3 shows the evolution of this mode mix in the launcher. Starting with only the $TE_{28,8}$ mode at z=0, the satellite modes are gradually produced as z increases, resulting in a sequence of peaked current contours corresponding to an rf beam bouncing off the interior walls along a helical path. The box in Fig. 3 represents the slot through which the rf beam is launched.

Our launcher was designed to operate close to cutoff in order to reduce its length and provide clearance for the electron beam. One concern with operation near cutoff was the possibility that the gyrotron interaction would continue beyond the cavity and into the launcher. However, nonlinear simulations indicate that the interaction does end early in the nonlinear uptaper of the cavity, primarily due to the drop-off in the magnetic field. Another concern was the possibility of spurious modes being excited in the launcher. However, we confirmed in our 110 GHz experiments that it is possible to design such a launcher so that it does not support high Q modes, and is therefore less susceptible to such oscillations.

The four mirror transmission line following the launcher is used to phase correct and focus the beam, and then launch the radiation through a side window. The transmission line also separates the radiation from the spent electron beam in the gyrotron, simplifying the design of the collector. This arrangement reduces the deleterious effects of reflections from the vacuum window, and provides better pumping conductance within the vacuum tube for quicker processing. Diffraction codes developed at M.I.T.[15] were used to design the internal mode converter, and an overall conversion efficiency of 93-95% was achieved. The final output is a circular Gaussian-like beam with a 2.8 cm waist at the 10 cm diameter window.

An important goal of this experiment was to optimize the electron gun design so that a high quality beam was produced over a wide range of operating parameters. Our 110 GHz gyrotron experiments[13] indicated that good beam quality is critical in achieving higher efficiency. Factors that can degrade beam quality include poor beam optics, cathode surface roughness[16], electrode machining errors and operation at high temperature. The 170 GHz gun was simulated with EGUN. The mesh size was carefully checked to ensure that the beam optics were accurately modeled. The electrode shapes were optimized so that the beam characteristics were insensitive to machining errors and to variations in the operating parameters resulting from misalignment or beam voltage fluctuations. Figure 4 shows one example of this optimization process. In this graph the dependence of the beam velocity ratio α on the cathode magnetic field is shown for three gun designs. All three designs could achieve the desired α value of 1.6-1.7 with low velocity spread. However, the design with α less sensitive to the cathode field was chosen. For this design a slight variation of magnetic field azimuthally around the emitter would result in a smaller variation of α, and therefore a lower beam velocity spread. Also shown in Fig. 4 is the predicted beam velocity ratio based on adiabatic theory[17]. Clearly adiabatic theory inadequately explains the dependence of α on the cathode field, especially below 1.85 kG.

Simulations of the final design of our 170 GHz gun indicated that the perpendicular velocity spread due to beam optics is 2.5% for a 35 A beam. Taking into account additional spreads, which includes 3.7% from the cathode surface roughness, 0.9% from misalignment, and 2.6% from the machining errors, the final beam spread was predicted to be 5-7%. Nonlinear simulations of the cavity based on this spread indicated that an operating efficiency of 35% would be feasible.

III. EXPERIMENTAL RESULTS

Although the overall goal of the M.I.T. program is to investigate the gyrotron configuration as shown in Fig. 2, the initial experiments were conducted without the internal mode converter. The results of these tests are presented in this section. The objectives of these experiments were to investigate the electron beam characteristics, and to determine if mode competition was adversely affecting the operation of the cavity. It was felt that by operating without an internal mode converter, the measurements would be easier to interpret. The rf power generated by the cavity was propagated by a 2.2 cm radius cylindrical copper waveguide along the tube axis to a quartz vacuum window. The launching of the $TE_{28,8}$ mode through the output window also allowed us to assess the performance of the mode converter externally to determine if it was functioning correctly.

These experiments were carried out with the gyrotron operating at 2 Hz with 3 μsec pulses. We began with low voltage operation, and verified that full beam transmission was being achieved. We then used beam interception on the beam scraper just before the cavity to adjust the tube in the magnet bore and center the beam in the cavity. Once we confirmed that the beam was centered and not scraping on any internal components, we operated the gyrotron at full voltage (80-100 kV) and swept the cathode and cavity magnetic fields to obtain a spectrum of modes. Thirteen modes were identified between 166 and 178 GHz, an indication of the dense spectrum of the cavity. The frequencies of these modes were measured to within 5 MHz using a harmonic mixer and digital scope with FFT capabilities. These frequencies agreed with predictions based on cold cavity theory to within ±50 MHz. This confirmed that the cavity had been built to the correct dimensions. The TE_{mp1} modes observed had radial indices p between 7 and 10, verifying that the beam was propagating through the center of the cavity.

We then investigated the operation of the gyrotron around the design frequency of 170 GHz. We found that the $TE_{27,8,1}$ at 166.6 GHz was easier to access than the $TE_{28,8,1}$, and focused our attention on that mode. Figure 5 shows the dependence of the output power and efficiency on the beam current. The power was measured with an 20 cm Scientech calorimeter that was modified to be 85-90% absorbing at these frequencies. At each beam current in Fig. 5 the cavity and cathode magnetic fields were optimized to maximize power. The shot-to-shot power stability was better than 10% at each operating point, and measurements using our harmonic mixer indicated single mode emission at all currents. Efficiencies over 30% were achieved for all currents over 15 A. Also shown is the optimized detuning parameter $\Delta=2(1-\omega_c/\omega)/\beta_\perp^2$, where $\omega_c=eB_o/\gamma mc$ is the cyclotron frequency and is calculated from the cavity magnetic field B_o, the relativistic factor γ, the rf frequency ω, and $\beta_\perp=v_\perp/c$. The increase in Δ as the beam current rises is consistent with nonlinear theory. The measured detuning value of 0.43 at 35 A is lower than the optimum theoretical value of 0.5 and may indicate that mode competition is preventing operation at magnetic fields that yield the highest efficiencies.

Although the $TE_{28,8,1}$ mode was a little more difficult to excite than the $TE_{27,8,1}$, we were able to achieve similar high powers in both modes. A comparison of operation at high current in these two modes can be seen in Fig. 6 for beam voltages between 83 and 87 kV. The results were nearly identical, which was expected because the coupling between the beam and rf field is similar for both modes. A maximum output power of 1.5 MW was measured in the $TE_{28,8,1}$ mode at 170.0 GHz with an 87 kV, 49 A beam for an efficiency of 35%. The velocity ratio of the electron beam was measured to be 1.4. When operating at the design point listed in Table I, 1.05 MW of output power was generated with an efficiency of 35%.

An interesting comparison can be made between the $TE_{27,8,1}$ operating points near 40 A in Figs. 5 and 6. This comparison is given in Table II. Both operating points, although quite different, produce 1.25 MW and an efficiency of about 35%. Although one might expect that operation at a higher velocity ratio (column 1) would yield a higher efficiency, the lower detuning (0.44) indicates that mode competition is limiting access to the high efficiency region. The operating point with lower α (column 2) has less energy available for microwave generation, but the higher detuning suggests this energy is being extracted more efficiently.

In order to better understand the severity of mode competition and multimoding in our experiment, a map of the observed modes was produced. Oscillations in a competing mode can result in a decrease of the interaction efficiency, degraded performance of the mode converter, and an increase in window reflections that can cause trapped power in the tube. This mode map was produced by varying the cathode and cavity magnetic fields, and is shown in Fig. 7. Varying the cathode field changes the beam velocity ratio, with lower field corresponding to higher α. Varying the cavity field allows one to optimize the detuning parameter Δ. The upper boundary of the region where modes are excited corresponds to a magnetic compression of about 35. Above this boundary the compression is less, resulting in a larger beam that partially intercepts the circuit between the gun and cavity. The other boundary, which corresponds to a compression of 40, indicates the region where electrons start to reflect back into the gun because α is too high. Between these two boundaries we primarily observed two rows of azimuthal TE_{mp1} modes with radial indices p of 8 and 9. Each row corresponds to a region of constant compression with a fixed beam radius R_e. For the upper row, the beam is larger and couples to modes closer to the cavity wall (i.e., modes with lower p). The observed sequences of azimuthal modes with the same radial index is consistent with the fact that the gyrotron coupling factor $J_{m\pm1}(k_\perp R_e)$ is a weak function of m when m>>1.

In general, our gyrotron was characterized by regions of single mode emission. Figure 7 indicates a few operating regions that resulted in multimoding, such as the boundary between the $TE_{24,8,1}$ and $TE_{25,8,1}$ modes. It is also evident that the $TE_{28,8,1}$ region of excitation is smaller than the regions of neighboring modes. This may be due to the fact that the window was matched to the $TE_{28,8,1}$ frequency of 170 GHz. For other modes at different frequencies, the window mismatch can cause reflection and raise the cavity Q, increasing the potential for exciting these modes. One indication that window reflections may be influencing the gyrotron's operation is shown in Fig.8. This graph shows the measured frequency while the detuning parameter was varied. The discrete jump of 70 MHz observed for the $TE_{27,8,1}$ mode is consistent with a window reflection[18]. For the $TE_{28,8,1}$ mode the frequency varies continuously, indicating no such reflection.

We also investigated the influence of startup on the operating behavior. It has been shown[19] that the way in which the operating point is reached can be used to eliminate undesirable modes and assure oscillation in the proper mode. Figure 9 shows the startup characteristics of the $TE_{27,8,1}$ mode as the cathode voltage was raised to 105 kV. The non-adiabatic behavior of the gun is clearly evident, with the oscillatory dependence of α on cathode voltage. Also shown are the theoretical starting current curves for the modes with the strongest coupling to the beam. No microwaves were observed up to 63 kV. At that point, the $TE_{29,8,1}$ was excited, consistent with the theoretical starting current. The excitation of higher frequency modes before the $TE_{27,8,1}$ is reached is consistent with the fact that the cyclotron frequency is higher at lower beam voltages. Note that each mode continued to oscillate beyond the region predicted by linear theory, an indication that the mode was operating in the hard excitation region.

The high power and efficiencies measured in this experiment indicate that the electron gun is producing a good quality beam with the expected characteristics. A more direct confirmation that the gun is operating as designed can be seen in Fig. 10. This graph shows the dependence of the velocity ratio on the cathode voltage. Measurements are compared with simulations based on EGUN. The velocity ratio was measured using a capacitive probe located directly in front of the cavity. This graph exhibits the same non-adiabatic behavior as was seen in Fig. 9. The experimental points deviate slightly from the theoretical predictions, but overall the agreement is good.

IV. CONCLUSIONS

The results of initial experiments on the M.I.T. 170 GHz megawatt gyrotron have been presented and indicate that the overall performance of the tube was excellent and consistent with theoretical predictions. Megawatt power levels with efficiencies between 30-35% were measured over a wide range of operating parameters for the $TE_{28,8,1}$ mode. Similar measurements were also obtained in the neighboring $TE_{27,8,1}$ mode at 166.6 GHz, and the $TE_{29,8,1}$ mode at 173.5 GHz.

These results demonstrate that efficiencies above 35% can be achieved in gyrotron cavities with v_{mp}>50 and represent a major achievement. Particularly encouraging was the fact that the high efficiencies could be maintained at the highest output powers, in contrast to some previous experiments where the efficiency tended to degrade at the higher beam currents. These results confirm that the careful design process has produced an electron gun with a high quality beam, and that the tapered cavity with an output iris is effective in reducing mode competition.

In the next phase of this experiment, the mode converter will be tested externally to confirm that it can efficiently produce a Gaussian beam. It will then be placed inside the gyrotron so that we can evaluate the performance of the combined cavity and mode converter. In later experiments we will explore the option of using the same gyrotron to produce discrete frequencies at 150, 170, and 190 GHz by varying the cavity magnetic field. These frequencies were chosen because they would be matched to the vacuum window. Simulations indicate that high beam quality, and cavity interaction efficiencies of 35%, should be possible over this frequency range. We will also investigate the use of a single-stage depressed collector that could increase the overall efficiency to 50%. As part of this study, we will study the role of trapped electrons and their effect of the performance of the gyrotron.

V. ACKNOWLEDGMENTS

The authors which to thank W.J. Mulligan and G.F. Yarworth for their help in the assembly of this experiment. They also wish to thank Kevin Felch and his colleagues at C.P.I. for their involvement in the construction of the electron gun, and Baruch Levush and Tom Antonsen at the

University of Maryland for their collaboration on the design of the cavity used in these experiments. This work was supported by U.S.D.O.E. contract DE-FC02-93ER54186.

VI. REFERENCES

[1] *Gyrotron Oscillators: Their Principles and Practice*, edited by C.J. Edgecombe (Taylor and Francis, London, 1993).

[2] K. Felch, M. Blank, P. Borchard, T.S. Chu, J. Feinstein, H.R. Jory, J.A. Lorbeck, C.M. Loring, Y.M. Mizuhara, J.M. Neilson, R. Schumacher, and R.J. Temkin, IEEE Trans. Plasma Science **24**, 558-569 (1996).

[3] M. Sato, T. Shimozuma, Y. Takita, S. Kubo, H. Idei, K. Ohkubo, T. Kuroda, T. Watari, M. Loring, S. Chu, K. Felch, and H. Huey, Proceedings of the Twentieth Int. Conf. Infrared and Millimeter Waves, Orlando, Florida, 1995, edited by R.J. Temkin, p. 195.

[4] G.G. Denisov, A.N. Kuftin, V.I. Malygin, N.P. Venediktov, D.V. Vinogradov, and V.E. Zapevalov, Int. Journal Electronics **72,** 1079-1091 (1992).

[5] S. Alberti, O. Braz, P. Garin, E. Giguet, M. Pain, P. Thouvenin, M. Thumm, C. Tran, and M.Q. Tran, Proceedings of the 21st Int. Conf. Infrared and Millimeter Waves, Berlin, Germany, 1996, edited by M. von-Ortenberg and H.U. Mueller, p. AF1.

[6] G. Dammertz, O. Braz, C.T. Iatrou, M. Kuntze, A. Mobius, B. Piosczyk, and M. Thumm, IEEE Trans. Plasma Science **24**, 570-578 (1996).

[7] V. Erckmann and U. Gasparino, Plasma Phys. and Controlled Fusion **36**, 1869 (1994).

[8] M. Makowski, IEEE Trans. Plasma Science **24**, 1023-1032 (1996).

[9] K.E. Kreischer, B.G. Danly, J.B. Schutkeker, and R.J. Temkin, IEEE Trans. Plasma Science, PS-13, 368 (1985).

[10] K. Kreischer, J. Schutkeker, B. Danly, W. Mulligan, and R. Temkin, Int. J. Electronics **57**, 835 (1984).

[11] K.E. Kreischer, T.L. Grimm, W.C. Guss, A.W. Mobius, and R.J. Temkin, Phys. Fluids **B2,** 640-646 (1990).

[12] T.L. Grimm, K.E. Kreischer, and R.J. Temkin Phys. Fluids **B5**, 4135-4143 (1993).

[13] K.E. Kreischer, M. Blank, B.G. Danly, T. Kimura, and R.J. Temkin, IEDM Technical Digest IEEE Cat. No. CH35706, p. 243-246 (1994).

[14] S.Y. Cai, T.M. Antonsen, G. Saraph, and B. Levush, Int. J. Electronics **72**, 759-777 (1992).

[15] M. Blank, K. Kreischer, and R.J. Temkin, IEEE Trans. Plasma Science **24,** 1058-1066 (1996).

[16] Y.Y. Lau, J. Applied Phys. **61,** 36 (1987).

[17] J.M. Baird and W. Lawson, Int. J. Electron. **61**, 953 (1986).

[18] K.E. Kreischer, B.G. Danly, P. Woskoboinikow, W.J. Mulligan, and R.J. Temkin, Int. J. Electronics **57**, 851-862 (1984).

[19] D.R. Whaley, M.Q. Tran, T.M. Tran, and T.M. Antonsen, Jr., IEEE Trans. Plasma Science **22**, 850-860 (1994).

Table I. M.I.T. 170 GHz gyrotron parameters

Mode	$TE_{28,8,1}$
Voltage (kV)	83
Current (A)	36
Velocity ratio	1.6
Efficiency (%)	35
Magnetic field (T)	6.7
Field compression	36
Cavity radius (cm)	1.69
Beam radius (cm)	0.83
L/λ	6.4
Diffractive Q	1300
Peak cavity loss (kW/cm^2)	2.1
Voltage depression (kV)	6.0

Table II. $TE_{27,8,1}$ operation at high power

Voltage (kV)	94	84
Current (A)	38.7	42.8
Power (MW)	1.25	1.25
Velocity ratio	1.94	1.43
Efficiency (%)	34.6	34.4
Magnetic field (T)	6.64	6.55
Detuning	0.44	0.59

FIGURE CAPTIONS

Figure 1 - The dependence of the TE mode index v_{mp} for a 170 GHz gyrotron on the output power and the peak ohmic losses in the cavity walls.

Figure 2 - Schematic of the MIT 170 GHz gyrotron.

Figure 3 - Intensity of the surface currents on the inside walls of the launcher. The contours represent the ratio of the local wall current to the current at the beginning of the launcher. The contours are plotted as a function of the axial distance z and the azimuthal angle ϕ.

Figure 4 - The dependence of the beam velocity ratio on the magnetic field at the cathode for three different designs.

Figure 5 - The measured output power, efficiency, and detuning parameter for the $TE_{27,8}$ mode after optimization of the cavity magnetic field.

Figure 6 - A comparison of the operating characteristics of the $TE_{27,8,1}$ and $TE_{28,8,1}$ modes at high current.

Figure 7 - A map of the observed modes as a function of the cathode and cavity magnetic fields.

Figure 8 - The change in output frequency as the cavity magnetic field was varied. The dotted line represents a discrete jump in frequency.

Figure 9 - A comparison of the modes observed during startup with predictions based on linear theory. The scan was done for a magnetic field of 6.77 T. The beam current varied from 21.2 A at 60 kV to 26.9 A at 104 kV.

Figure 10 - A comparison of the beam velocity ratio as measured with a capacitive probe with predictions based on EGUN.

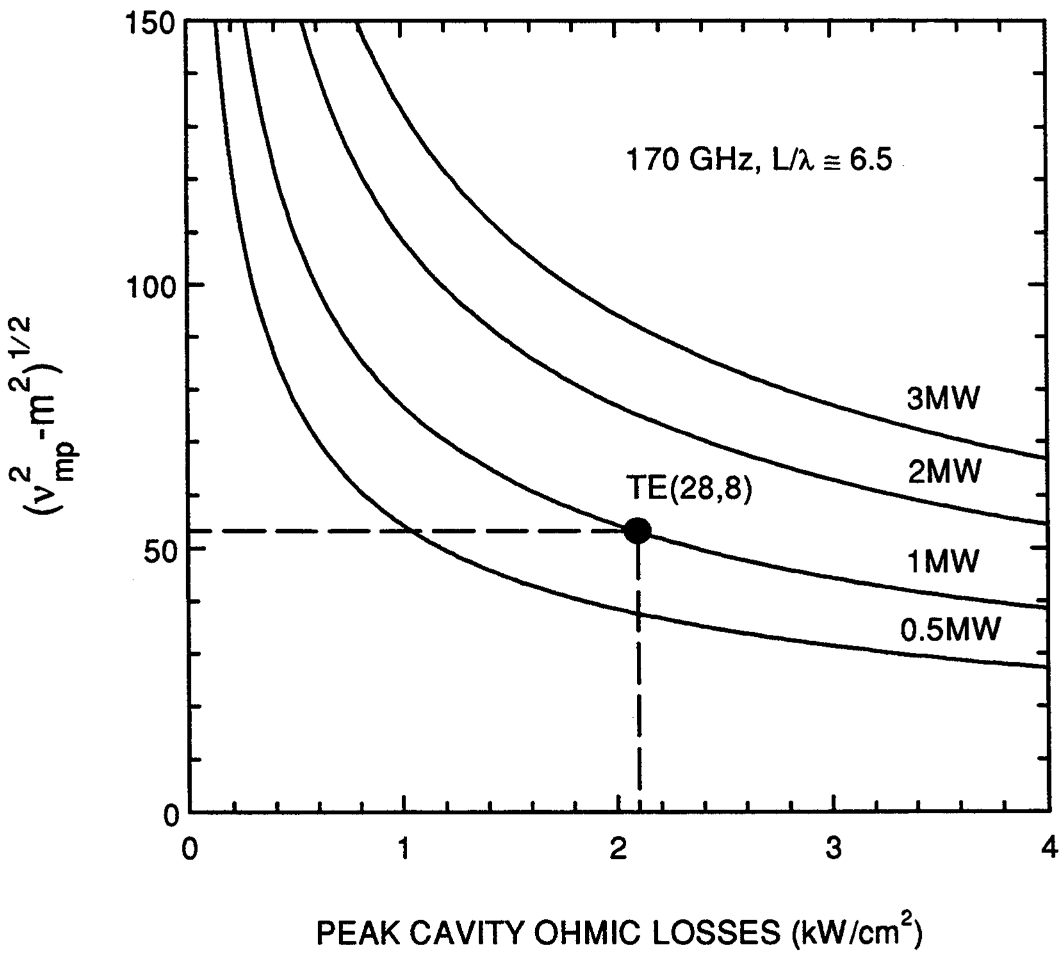
150
100
50
0
0
1
2
3
4
170 GHz, L/λ ≅ 6.5
3MW
2MW
TE(28,8)
1MW
0.5MW
$(\nu_{mp}^2 - m^2)^{1/2}$
PEAK CAVITY OHMIC LOSSES (kW/cm^2)

Figure 1

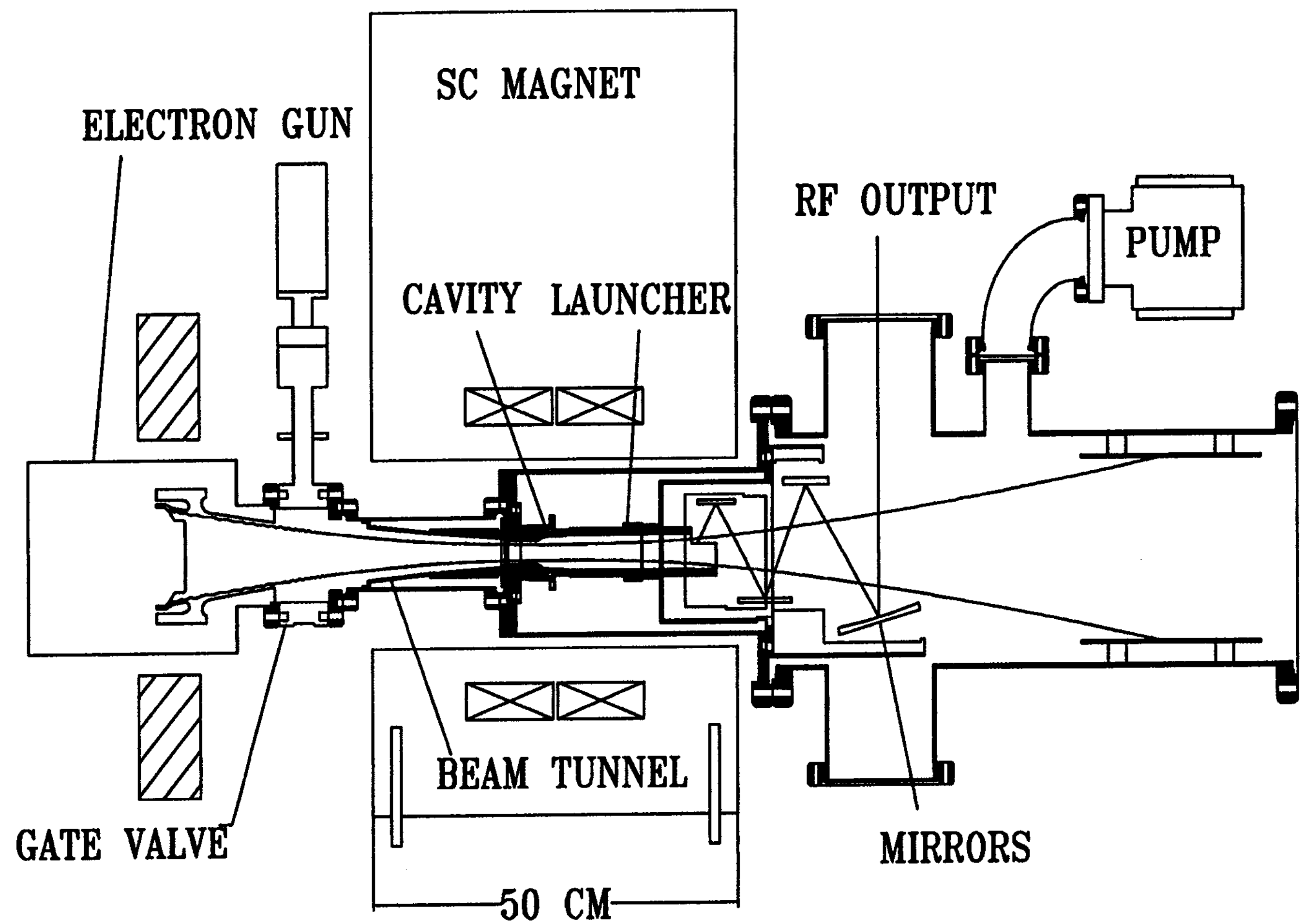
SC MAGNET
ELECTRON GUN
CAVITY LAUNCHER
RF OUTPUT
PUMP
BEAM TUNNEL
GATE VALVE
MIRRORS
50 CM

Figure 2

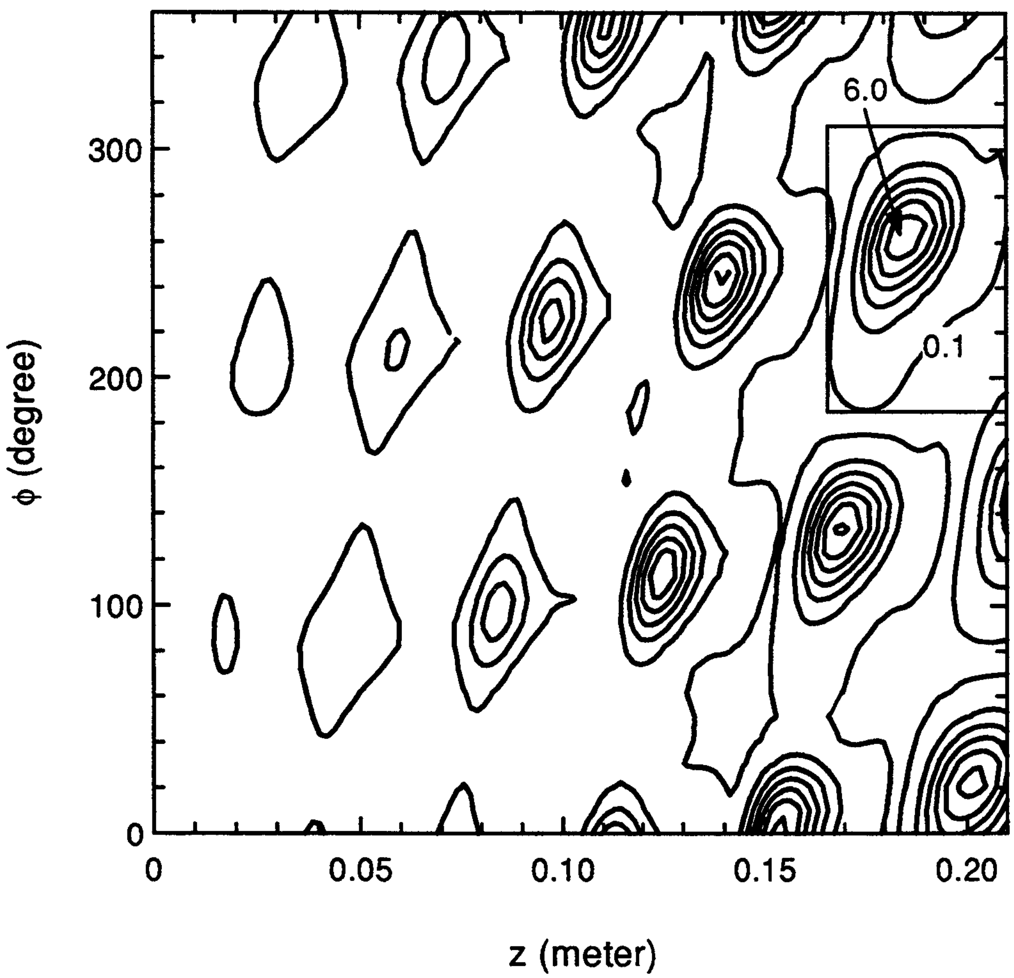

Figure 3

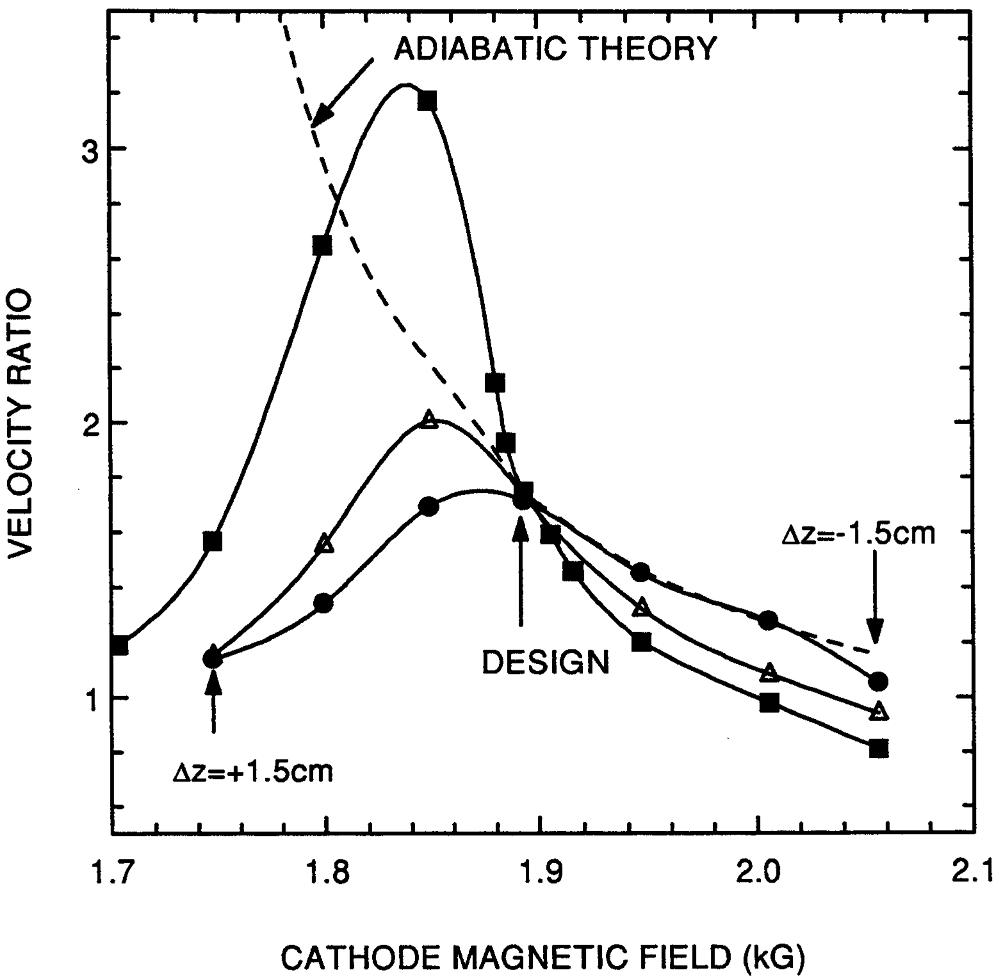
ADIABATIC THEORY
VELOCITY RATIO
3
2
1
Δz=-1.5cm
DESIGN
Δz=+1.5cm
1.7
1.8
1.9
2.0
2.1
CATHODE MAGNETIC FIELD (kG)

Figure 4

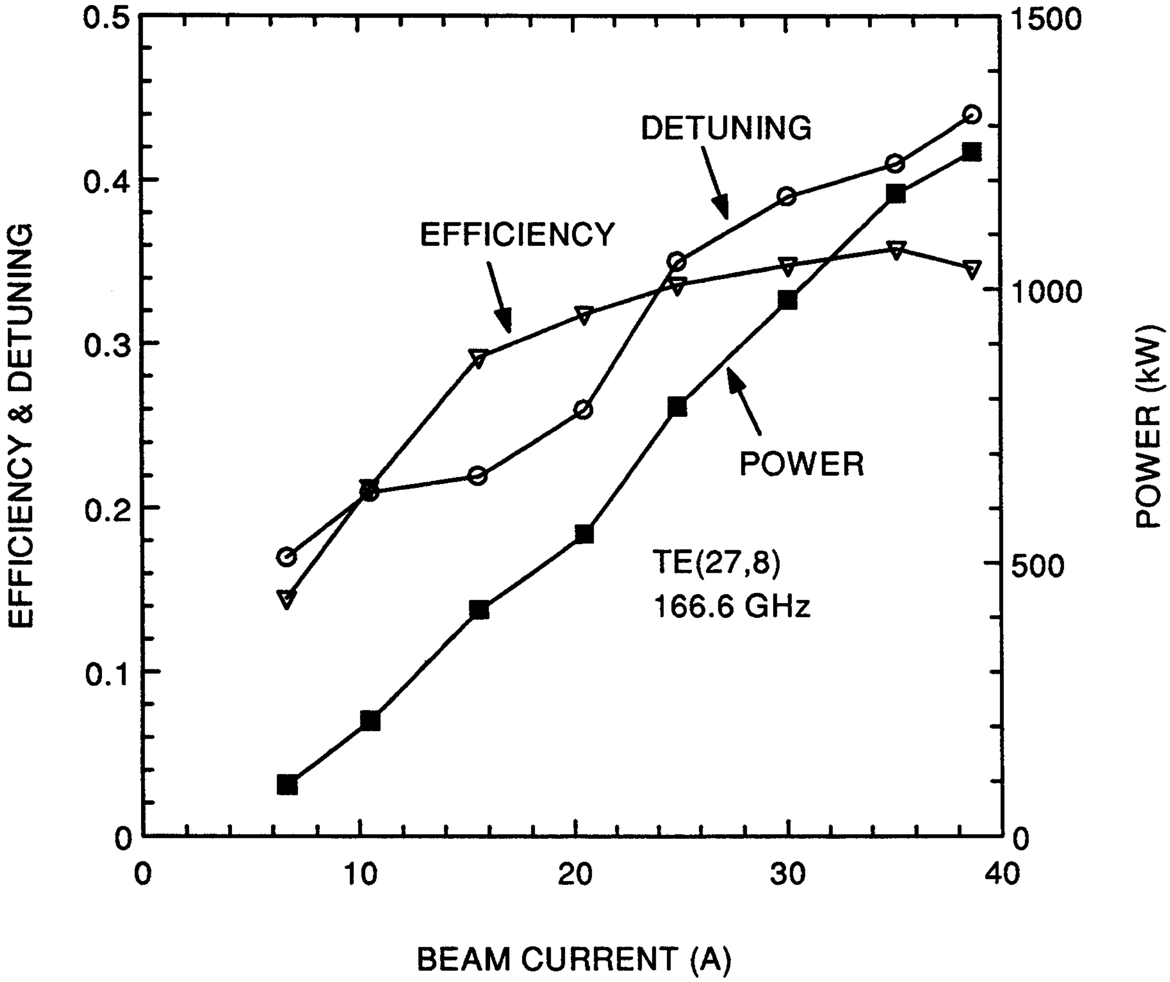
0.5
0.4
0.3
0.2
0.1
0
1500
1000
500
0
0
10
20
30
40
DETUNING
EFFICIENCY
POWER
TE(27,8)
166.6 GHz
EFFICIENCY & DETUNING
POWER (kW)
BEAM CURRENT (A)

Figure 5

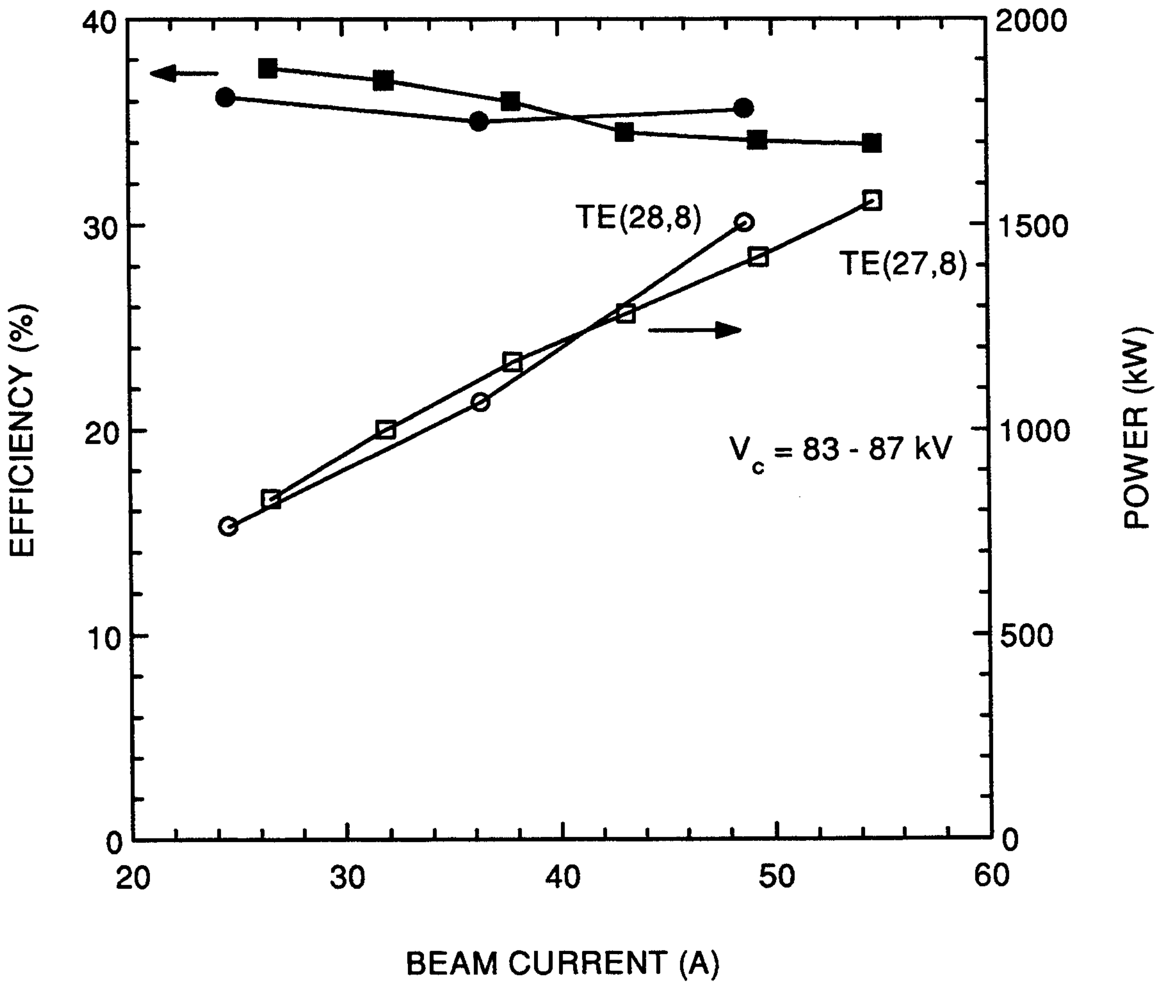

40
30
20
10
0
2000
1500
1000
500
0
20
30
40
50
60
EFFICIENCY (%)
POWER (kW)
BEAM CURRENT (A)
TE(28,8)
TE(27,8)
V_c = 83 - 87 kV

Figure 6

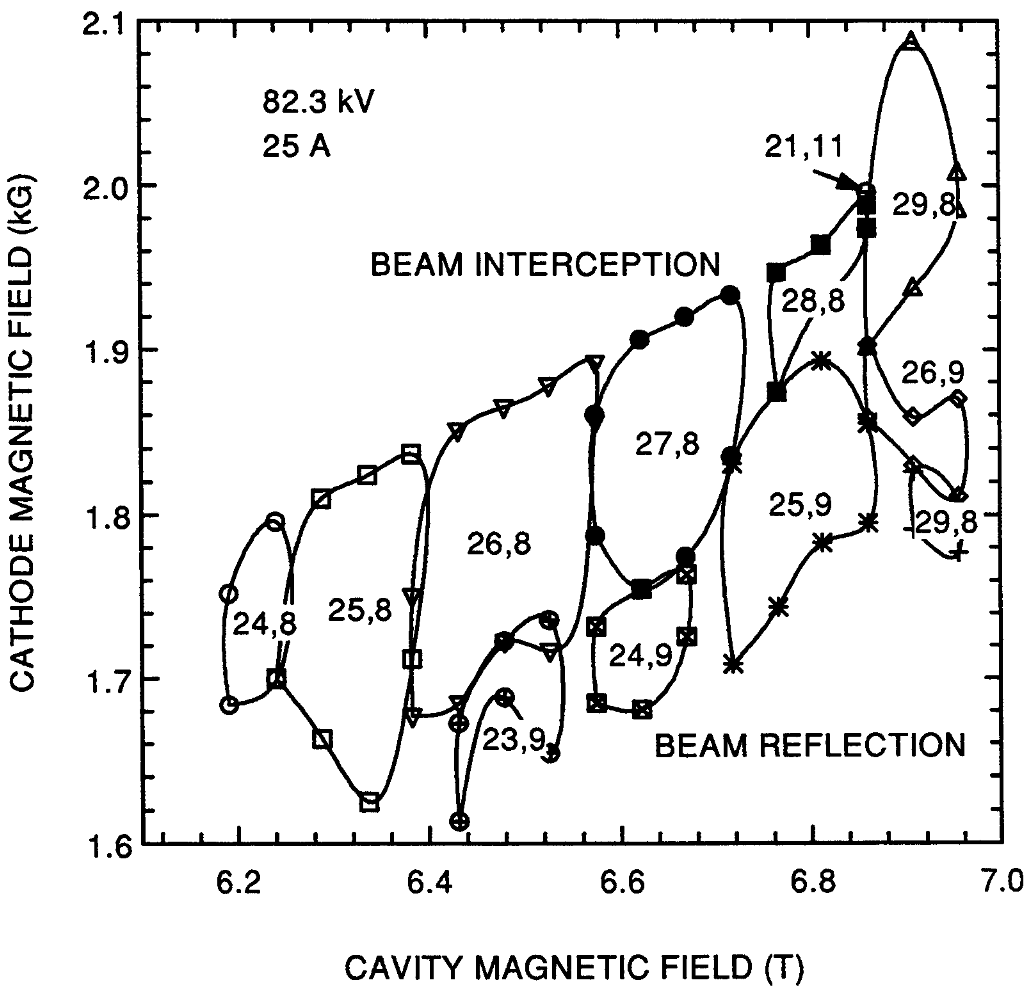
82.3 kV
25 A
21,11
29,8
BEAM INTERCEPTION
28,8
26,9
27,8
25,9
29,8
26,8
24,8
25,8
24,9
23,9
BEAM REFLECTION
CATHODE MAGNETIC FIELD (kG)
CAVITY MAGNETIC FIELD (T)
2.1
2.0
1.9
1.8
1.7
1.6
6.2
6.4
6.6
6.8
7.0

Figure 7

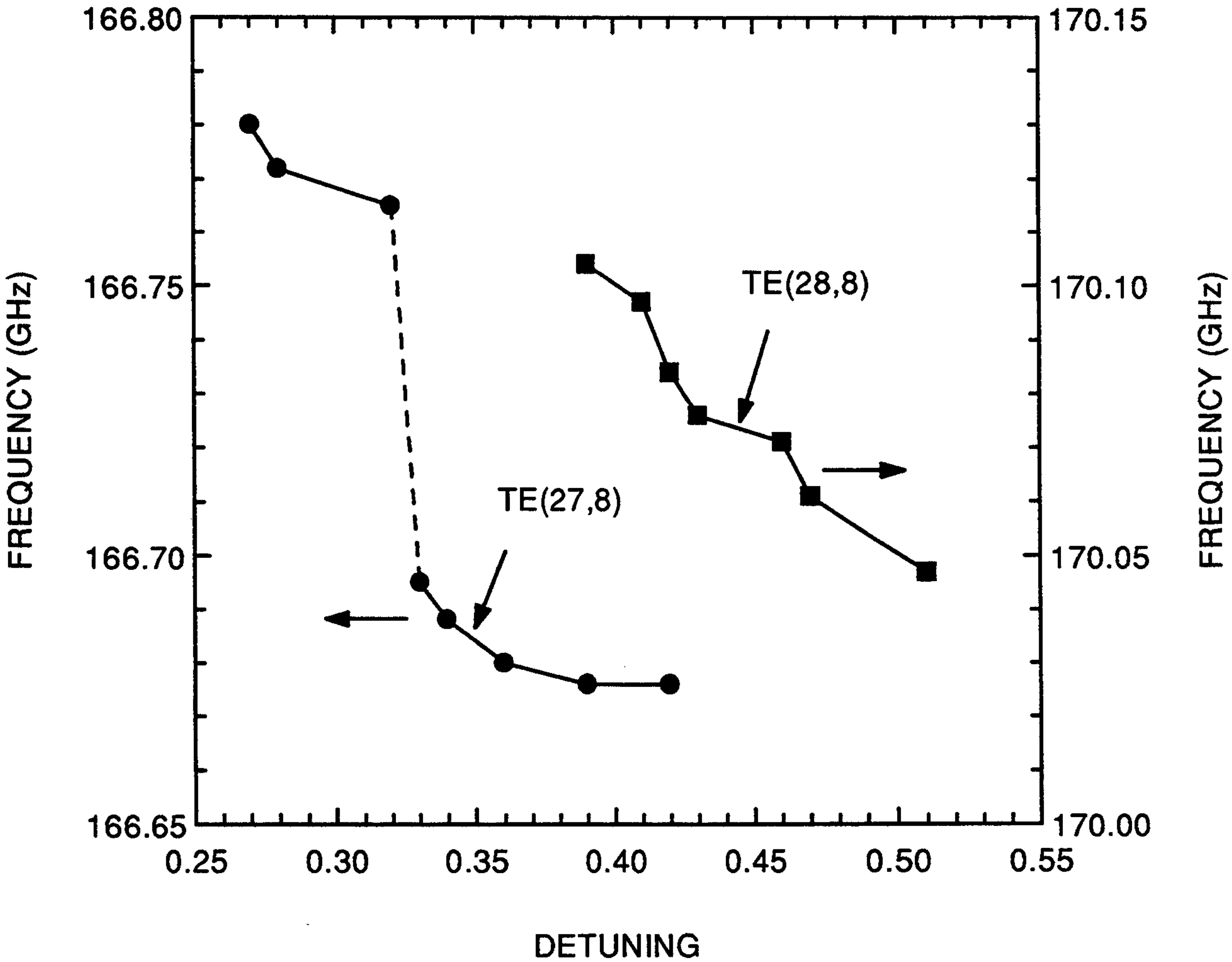

166.80
166.75
166.70
166.65
170.15
170.10
170.05
170.00
0.25
0.30
0.35
0.40
0.45
0.50
0.55
FREQUENCY (GHz)
FREQUENCY (GHz)
DETUNING
TE(28,8)
TE(27,8)

Figure 8

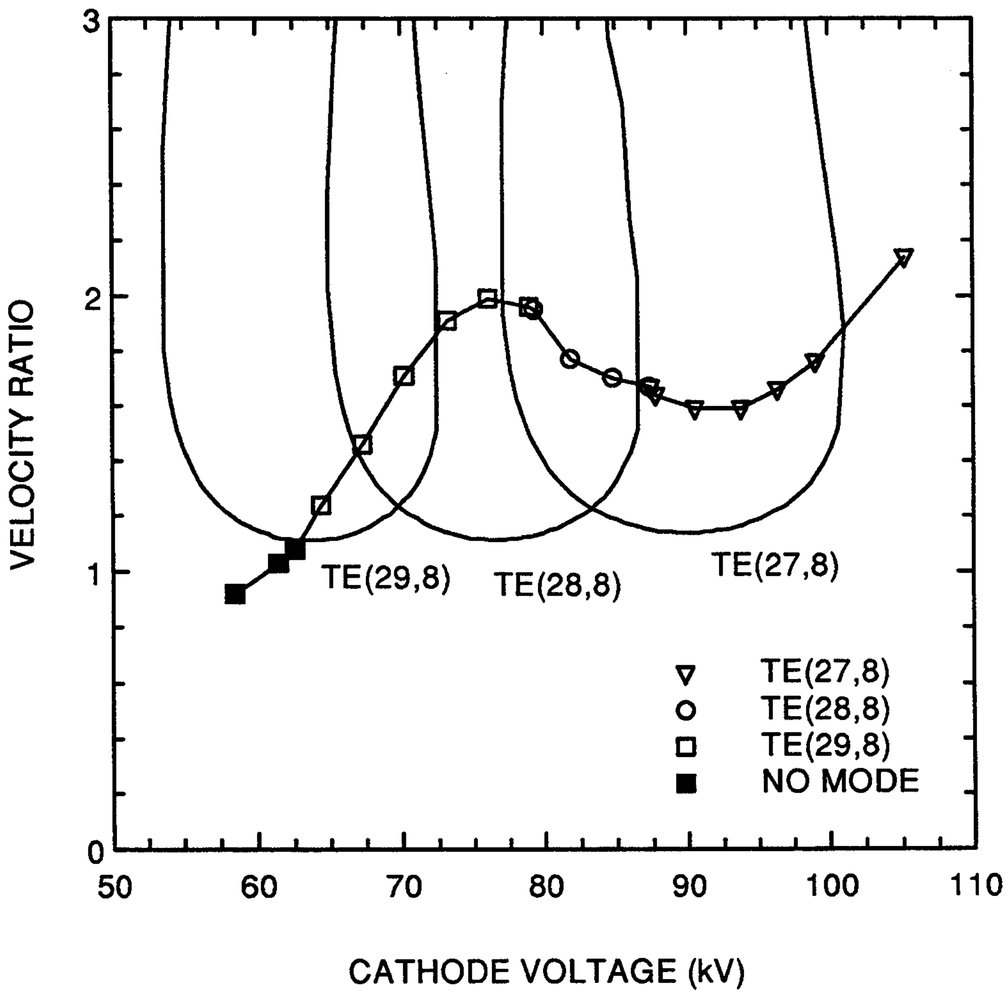
3
2
1
0
50
60
70
80
90
100
110
VELOCITY RATIO
CATHODE VOLTAGE (kV)
TE(29,8)
TE(28,8)
TE(27,8)
TE(27,8)
TE(28,8)
TE(29,8)
NO MODE

Figure 9

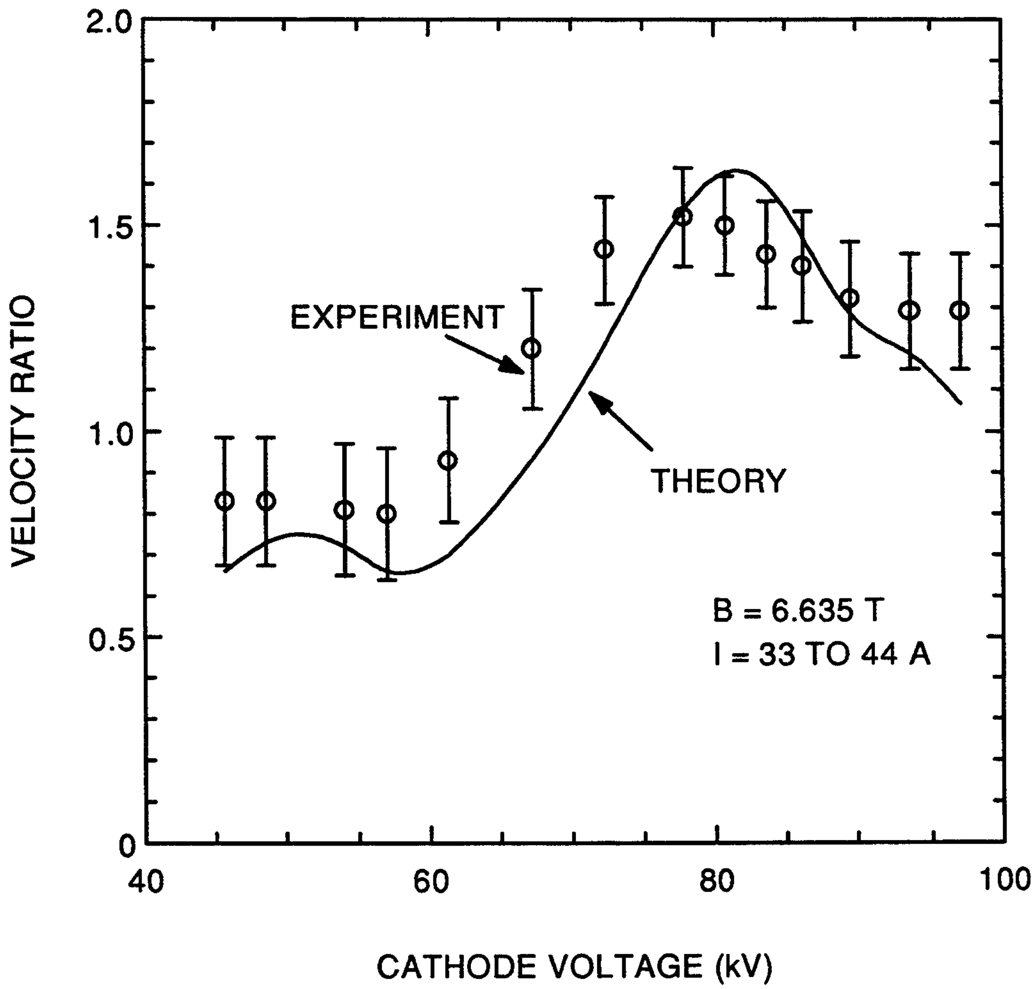
2.0
1.5
1.0
0.5
0
40
60
80
100
VELOCITY RATIO
CATHODE VOLTAGE (kV)
EXPERIMENT
THEORY
B = 6.635 T
I = 33 TO 44 A

Figure 10